Ab initio determination of local coupling interaction in arbitrary nanostructures: Application to photonic crystal slabs and cavities

Gengyan Chen, Yi-Cong Yu, Xiao-Lu Zhuo, Yong-Gang Huang, Haoxiang Jiang, Jing-Feng Liu, Chong-Jun Jin, and Xue-Hua Wang

Phys. Rev. B **87**, 195138 — Published 28 May 2013

DOI: 10.1103/PhysRevB.87.195138

Ab-initio Determination of Local Coupling Interaction in Arbitrary Nanostructures: Application to Photonic Crystal Slabs and Cavities

Gengyan Chen, Yi-Cong Yu, Xiao-Lu Zhuo, Yong-Gang Huang†,
Haoxiang Jiang, Jing-Feng Liu‡, Chong-Jun Jin, and Xue-Hua Wang*

State Key Laboratory of Optoelectronic Materials and Technologies, School of Physics and Engineering, Sun Yat-sen University, Guangzhou 510275, China

ABSTRACT

We develop a local coupling theory to simultaneously treat the weak and strong interaction between a quantum emitter and photons in arbitrary nanostructures. The local coupling strength proportional to the projected local density of states (PLDOS) for photons is determined by a flexible and efficient method. The recent experimental observation for the photonic crystal slabs is very well interpreted by our *ab-initio* PLDOS, while the scaling invariant law is found to be inapplicable for these PC slabs. More importantly, a bridge linking the PLDOS and cavity quantum electrodynamics is established by the local coupling strength to account for quality factor, g factor and vacuum Rabi splitting. Our work enriches the knowledge about the light-matter interaction in nanostructures.

PACS numbers: 42.50.Ct, 42.70.Qs, 42.50.Pq , 78.67.Pt

I. INTRODUCTION

Controlling the interaction between a quantum emitter and photons at the nanoscale has been central subject of nano-optics with intense activities including modification of spontaneous emission (SE) rates[1-10], vacuum Rabi splitting[11-13], lasing under strong coupling[14], single-photon source[15] and Anderson localization[16]. The interaction may be characterized by the local coupling strength (LCS)[17, 18] proportional to the projected local density of states (PLDOS)[19, 20]. Hence tailoring the PLDOS plays a key role in controlling the interaction at the nanoscale.

Due to its pivotal role, probing the PLDOS via the SE rate in various nanostructures has recently received special attention, such as photonic crystal (PC)[10], random photonic media[21], disordered metal film[22], metal nanowires[23] and PC slab[24]. However, the quantitative theoretical explanations for the results have been still lacking due to the challenge of simulating the PLDOS in arbitrary nanostructures. Furthermore, this probe approach is valid only in the weak coupling between a quantum emitter and photons. In this case, the SE rate is just equal to the LCS at the transition frequency of the quantum emitter[17], and then the PLDOS can be obtained from the SE rate by the proportional relation between them.

On the other hand, the solid-state cavity quantum electrodynamics (CQED) systems with strong coupling between a quantum emitter and cavity mode have been a research focus, because they not only provide test beds for fundamental quantum physics but also have important applications in quantum information processing[11, 12, 25-27]. In strong coupling regime, the SE rate cannot describe this dynamic process, and the above-mentioned probe approach of the PLDOS is hence invalid. Certainly, it is a vital demand to establish a linking bridge between the PLDOS and the CQED both for the probe of the PLDOS and for the manipulation of the quantum nature of solid-state CQED in the strong coupling regime. Up to now, the linking bridge is still an open question.

Motivated by the above-mentioned vital challenge and demand, we develop a local

coupling theory to simultaneously treat the weak and strong interaction between a quantum emitter and photons in arbitrary nanostructures. The LCS is determined by the *ab-initio* mapping of the PLDOS based upon a flexible and efficient method. Our *ab-initio* PLDOS for the PC slab samples recently investigated by Wang *et al.*[24] agrees well with the probed PLDOS, while the scaling invariant law is not applicable to explain the experimental observation. We also demonstrate that the PC slabs have no gap inhibition effect when the transition dipole moment is normal to the slab. More importantly, we establish a linking bridge between the PLDOS and the CQED by the LCS to directly determine the quality factor, g factor and vacuum Rabi splitting which characterize the CQED. The measured results in the pioneering experiment on the solid-state strong-coupling system between a quantum dot and the PC L3 cavity [11] are reproduced from the *ab-initio* PLDOS.

The paper is organized as follows: In Sec. II, the theory and method for the local coupling interaction in arbitrary nanostructures are presented. The *ab-initio* simulated results for the PC slab and cavity are given in Sec. III. Finally, a brief conclusion remains in Sec. IV.

II. THEORY AND METHOD

A. The relation between the LCS and PLDOS

The interaction between photons and a two-level quantum emitter in nanostructures is characterized by LCS as[17, 18]:

$$\Gamma(\mathbf{r}_0,\omega) = 2\pi\sum_{\lambda}\left|g_{\lambda}(\mathbf{r}_0)\right|^2\delta(\omega-\omega_{\lambda}) \tag{1}$$

where $g_{\lambda}(\mathbf{r}_0) = i\omega_0(2\varepsilon_0\hbar\omega_{\lambda})^{-1/2}\,\mathbf{d}\cdot\mathbf{E}_{\lambda}(\mathbf{r}_0)$ is the coupling coefficient; $\mathbf{r}_0$, ω_0 and $\mathbf{d} = d\hat{\mathbf{d}}$ are the location, transition frequency and transition dipole moment of the quantum emitter; ω_{λ} and $\mathbf{E}_{\lambda}(\mathbf{r})$ are the frequency and electric field of the λ-th eigenmode in the nanostructure. Noticing the PLDOS defined as [19, 20]

$$\rho\left(\mathbf{r}_0,\omega,\hat{\mathbf{d}}\right)=\sum_{\lambda}\left|\hat{\mathbf{d}}\cdot\mathbf{E}_{\lambda}\left(\mathbf{r}_0\right)\right|^2\delta\left(\omega-\omega_{\lambda}\right), \tag{2}$$

and the property of δ function, it is straightforward to rewrite the LCS as:

$$\Gamma\left(\mathbf{r}_0,\omega\right)=\Gamma_0\frac{\omega}{\omega_0}M\left(\mathbf{r}_0,\omega,\hat{\mathbf{d}}\right). \tag{3}$$

Here $M\left(\mathbf{r}_0,\omega,\hat{\mathbf{d}}\right)=\rho\left(\mathbf{r}_0,\omega,\hat{\mathbf{d}}\right)/\rho_0(\mathbf{r}_0,\omega)$ is multiplication factor of the PLDOS, i.e. the normalized PLDOS to the density of states $\rho_0(\mathbf{r}_0,\omega)=\omega^2/3\pi^2c^3$ in vacuum; $\Gamma_0=\omega_0^3d^2/3\pi\hbar\varepsilon_0c^3$ is the SE rate of quantum emitter in vacuum.

B. The nonlocal and local effect of the interaction in frequency domain

As soon as the LCS is determined, the time evolution of the excited state of the quantum emitter can be obtained by[17, 18]:

$$C_e(\mathbf{r}_0,t)=\int_{-\infty}^{+\infty}C_e\left(\mathbf{r}_0,\omega\right)e^{-i\omega t}d\omega \tag{4}$$

where $C_e(\mathbf{r}_0,\omega)$ is the evolution spectrum of the excited state of the quantum emitter as [17, 18]:

$$C_e\left(\mathbf{r}_0,\omega\right)=\frac{1}{\pi}\frac{\Gamma\left(\mathbf{r}_0,\omega\right)/2}{\left[\omega-\omega_0-\Delta\left(\mathbf{r}_0,\omega\right)\right]^2+\left[\Gamma\left(\mathbf{r}_0,\omega\right)/2\right]^2}. \tag{5}$$

with the level shift of the quantum emitter due to its interaction with photons as [17, 18]:

$$\Delta\left(\mathbf{r}_0,\omega\right)=\frac{\mathcal{P}}{2\pi}\int_0^{\infty}\frac{\Gamma\left(\mathbf{r}_0,\omega'\right)}{\omega-\omega'}d\omega' \tag{6}$$

where $\mathcal{P}$ denotes integral principal value.

Traditionally, the LCS in Eq.(1) and Eq.(3) is often misunderstood as the SE rate of a quantum emitter at its excited state. In fact, the LCS characterizes the interaction of the quantum emitter with the photon modes *at any frequency*, valid in weak, medium

and strong coupling regime. It implies those photon modes with different frequencies from the transition frequency ω_0 can make contribution to quantum optics properties, as shown in Eq.(5). In other words, the interaction is "nonlocal" in frequency domain.

Only in the weak coupling regime, $\Gamma(\mathbf{r}_0,\omega)$ and $\Delta(\mathbf{r}_0,\omega)$ in Eq.(5) are slowly varying functions of frequency and can be approximately replaced by $\Gamma(\mathbf{r}_0,\omega=\omega_0)$ and $\Delta(\mathbf{r}_0,\omega=\omega_0)$. Hence Eq.(5) becomes a typical Lorentz line shape. In this case, the photon modes at $\omega=\omega_0$ dominate the contribution to the interaction and the LCS $\Gamma(\mathbf{r}_0,\omega=\omega_0)$ can be regarded as the SE rate. Therefore, the SE lifetime of the quantum emitter in the weak coupling regime can be expressed as [17]:

$$\tau(\mathbf{r}_0)=\frac{1}{\Gamma(\mathbf{r}_0,\omega_0)}=\frac{\tau_0}{M\left(\mathbf{r}_0,\omega_0,\hat{\mathbf{d}}\right)} \tag{7}$$

where τ_0 is the SE lifetime of the quantum emitter in vacuum. Apparently, the multiplication factor $M\left(\mathbf{r}_0,\omega_0,\hat{\mathbf{d}}\right)$ of the PLDOS at $\omega=\omega_0$ in weak coupling regime is reduced to Purcell factor[1]. $\Gamma(\mathbf{r}_0,\omega_0)$ in Eq. (7) represents that the radiative lifetime of the quantum emitter is determined only by these photon modes at its transition frequency ω_0 (not including the nonradiative processes' contribution). This implies that the interaction is "local" in frequency domain in the weak coupling regime. Eq.(7) is the theoretical basis of experimentally probing the PLDOS in various nanostructures.

C. The linking bridge between the PLDOS and the CQED

For the solid-state CQED systems with strong coupling interaction, there is reversible exchange of a single photon between the quantum emitter and cavity mode. The SE rate can no longer describe this dynamic process, and the above-mentioned

probe approach of the PLDOS is invalid. It is significant to establish a linking bridge between the PLDOS and the CQED by the LCS.

Apparently, the LCS in an ideal single-mode cavity without loss is

$$\Gamma(\mathbf{r}_0,\omega)=2\pi\left|g_c(\mathbf{r}_0)\right|^2\delta(\omega-\omega_c), \tag{8}$$

where ω_c is the frequency of cavity mode, $\left|g_c(\mathbf{r}_0)\right|$ is the g factor. For the realistic cavity with the loss rate $\kappa=\omega_c/Q$ (Q is the quality factor), the LCS may be reasonably assumed with Lorentz line shape[28]:

$$\Gamma(\mathbf{r}_0,\omega)=2\left|g_c(\mathbf{r}_0)\right|^2\frac{\kappa/2}{(\omega-\omega_c)^2+(\kappa/2)^2}. \tag{9}$$

The rationality of the assumption lies in that Eq.(9) can reduce to Eq.(8) when $\kappa\to 0$, and in our following numerical simulation.

For a cavity with high quality factor and at resonance with the quantum emitter, from Eq.(3) and (9), we obtain

$$M\left(\mathbf{r}_0,\omega,\hat{\mathbf{d}}\right)=\frac{2\left|g_c(\mathbf{r}_0)\right|^2}{\Gamma_0}\frac{\kappa/2}{(\omega-\omega_c)^2+(\kappa/2)^2}. \tag{10}$$

By fitting the simulated $M\left(\mathbf{r}_0,\omega,\hat{\mathbf{d}}\right)$ with Lorentz function of Eq.(10), we can directly determine the mode frequency ω_c, decay rate κ and quality factor Q. The g factor can be obtained by the peak value $M_{peak}=M\left(\mathbf{r}_0,\omega=\omega_c,\hat{\mathbf{d}}\right)$ as:

$$\left|g_c(\mathbf{r}_0)\right|=\frac{1}{2}\sqrt{\Gamma_0\kappa M_{peak}} \tag{11}$$

From dressed-atom state[18], we can further derive vacuum Rabi splitting

$$\Omega=2\sqrt{\left|g_c(\mathbf{r}_0)\right|^2-(\frac{\kappa}{2})^2} \tag{12}$$

Eqs.(10)-(12) enable us directly to obtain the parameters characterizing the CQED from the normalized PLDOS. It is worthy of pointing out that the linking bridge presented here is valid for those nanostructures with the normalized PLDOS of the Lorentz line shape. In some open structures, e.g. the two close metallic nanospheres, it is possible to realize the strong coupling, but their PLDOS, which can be calculated

by our following simulation method, can't be fitted by Lorentz function. In this case, this simple linking bridge can't be adopted and we have to adopt Eqs. (4)-(6) to investigate the quantum optics properties.

D. Simulation method for the PLDOS

No matter in weak or strong coupling regime, the PLDOS plays a key role in governing the nano quantum optics properties. Various methods, such as Green function method[29], Brillouin zone method[30, 31] and finite difference time domain (FDTD) method[32-35], have been proposed to simulate the PLDOS for exploring the enhancement and inhibition effects on the SE in PCs. But the fast and efficient simulation of the PLDOS in arbitrary nanostructures has been still a challenge[34, 35]. The following method and technique are developed to overcome this challenge.

The PLDOS can be expressed by dyadic Green's function as[19, 36]

$$\rho\left(\mathbf{r}_0,\omega,\hat{\mathbf{d}}\right)=\frac{2\omega}{\pi c^2}\,\mathrm{Im}\left\{\hat{\mathbf{d}}\cdot\vec{\mathbf{G}}\left(\mathbf{r}_0,\mathbf{r}_0,\omega\right)\cdot\hat{\mathbf{d}}\right\}. \tag{13}$$

From Maxwell equations, the electric field induced by an oscillating point-dipole $\mathbf{d}=de^{-i\omega t}\hat{\mathbf{d}}$ at $\mathbf{r}_0$ is $\mathbf{E}_{\mathrm{d}}\left(\mathbf{r},\omega\right)=\mu_0\omega^2\vec{\mathbf{G}}\left(\mathbf{r},\mathbf{r}_0,\omega\right)\cdot d\hat{\mathbf{d}}$ [37, 38]. This implies the PLDOS can be calculated by:

$$\rho\left(\mathbf{r}_0,\omega,\hat{\mathbf{d}}\right)=\frac{2\varepsilon_0}{\pi\omega}\,\mathrm{Im}\left\{\frac{\hat{\mathbf{d}}\cdot\mathbf{E}_{\mathrm{d}}\left(\mathbf{r}_0,\omega\right)}{d}\right\}. \tag{14}$$

This can simplify the calculation of the PLDOS because the electric field of an oscillating point-dipole can be flexibly and efficiently simulated by various numerical methods, such as multiple scattering method, finite element method and FDTD method. More importantly, only the electric field at the dipole location needs to be stored and processed, which can save computer time and memory. It is noted that Eq.(14) can easily reduce to results for 1D and 2D cases in Ref. 39.

Usually in FDTD method, a Gaussian pulse as the point-dipole source is introduced [37-39] to simulate the time evolution of the electric field $\mathbf{E}_{\mathrm{d}}\left(\mathbf{r}_0,t\right)$ from the

point-dipole, then $\mathbf{E}_{\mathrm{d}}(\mathbf{r}_0,\omega)$ is obtained by Fourier transformation of $\mathbf{E}_{\mathrm{d}}(\mathbf{r}_0,t)$. But this is extremely time-consuming because Fourier transformation requires very long-time data to obtain convergent results. To accelerate the calculation, we adopt Pade approximation with Baker's algorithm[40] instead of Fourier transformation. Especially, the Pade approximation is very efficient for the nanostructures with highly localized field distribution, such as nano-cavities. Our test for the PC L3 cavity shows the Pade approximation can save computation time by about 200 times than Fourier transformation.

The mapping of the PLDOS in the present work is based on the local electrodynamics. For much smaller structures down to a few nanometers, the nonlocal effect has to be considered. Although we can simulate nonlocal electrodynamics by FDTD method [41, 42], this is beyond the scope of this paper.

Firstly, we verify our method by calculating the PLDOS in the vacuum with a silver nanosphere with radius 20nm. The distance between the piont-dipole and the nanosphere centre is 25nm. The dipole orientation is along radial direction. The frequency-dependent dielectric permittivity of silver is obtained by interpolating the experimental data[43]. FIG.1 shows $M(\mathbf{r}_0,\omega,\hat{\mathbf{d}})$ numerically calculated by Eq.(14) agrees with that obtained by Mie scattering theory[44], which validates our method. The red line is obtained by COMSOL software with the finite element method, rather than with FDTD method. This example also shows that our method is very flexible.

III. RESULTS AND DISCUSSIONS

A. The PLDOS in photonic crystal slabs

Recently, many experiments were reported in probing the PLDOS via the SE lifetime in various nanostructures[10, 21-24] according to Eq.(7). But the quantitative theoretical explanations are still lacking due to the difficulty in theoretical mapping of the PLDOS. We now apply our method to map out the *ab-initio* PLDOS in the

experimental PC slab samples[24], as shown in FIG. 2.

Wang *et al.* [24] used single self-assembled InGaAs quantum dot as internal probes to obtain the PLDOS in GaAs PC slabs. The lattice constant a ranges from 200 to 385 nm in a step of 5 nm and the air-hole radius is r=0.3a, while the slab thickness is fixed at d=154nm. Only quantum dots with the emission wavelength of 970±5 nm were selected to measure their radiative lifetime, at which wavelength the refractive index of GaAs is n=3.5. The experiment is very ingenious to exclude the contributions from nonradiative recombination and spin-flip processes. They also tried to interpret their experimental results based upon the scaling invariant law from the PLDOS of a PC slab sample, which will be shown to be invalid.

FIG. 3 shows $M\left(\mathbf{r}_0,\omega,\hat{\mathbf{d}}\right)$ for four different positions $\mathbf{r}_0$ in the PC slabs with three different lattice constants. $M\left(\mathbf{r}_0,\omega,\hat{\mathbf{d}}\right)$ in each slab change greatly for different positions, which means the PLDOS and the SE lifetime of the quantum dot in the PC slabs are strongly dependent on the position[17]. In each slab, there is a drop within the same normalized frequency range for different positions, which corresponds to the photonic band gap of each PC slab where the PLDOS is strongly suppressed. For three different PC slabs, the transition frequency of quantum dot is below, inside and above the individual band gap, respectively. This indicates the enhancement or inhibition of the SE can be controlled by adjusting the lattice constant.

However, the widths and positions of the band gaps for the three slabs are different. The band gap shifts to high normalized frequency with increasing lattice constant. This implies that the scaling invariant law does not work. According to Maxwell equations[45], only when a dielectric structure varies by similar transformation, the scaling invariant law is valid. Therefore, for the PC slabs with different lattice constants, the scaling invariant law requires that the normalized air-hole radius r/a and the normalized slab thickness d/a remain unchanged. For the PC slab samples[24], since the slab thickness is fixed at d=154nm, the normalized slab thickness d/a decreases as the lattice constant increases. As a result, the band gap should shift to the high

normalized frequency[46], rather than keeping unchanged. Therefore, the experimental results cannot be explained by the scaling invariant law from the PLDOS of a PC slab sample. Strictly, the dispersion relation of GaAs should be considered to obtain FIG. 3. But within the measured wavelength scope of the experiments, the refractive index can be regarded as a constant.

In order to understand the experimental results in Ref. 24, we calculate the PLDOS at the transition wavelength of 970nm for the PC slab samples with the lattice constant increasing from 200nm to 385nm by a step of 10nm. The results are shown in FIG. 4 for x- and y-orientations, respectively. In each PC slab, we find the maximum and minimum PLDOS values denoted by the dots on the two solid-lines, and also show other PLDOS values for four random locations denoted by the dots between the two solid-lines. The unit of the PLDOS is taken as $4/3a^2c$ for comparing with the probed PLDOS in FIG. 2 of Ref.24. From FIG. 4, we observe the drops in a wide range of normalized frequency. This width of the drop is larger than the band gaps for individual slab in FIG. 3. Obviously, the drops in FIG. 4 reflect the total gap effect of all slab samples, and agree well with the experimental results[24].

We further investigate the orientation-dependent character of the PLDOS and the SE lifetime. We choose the PC slab with a=290nm where the transition wavelength of quantum dot is inside the band gap as shown in FIG. 3(b), and calculate $M\left(\mathbf{r}_0,\omega,\hat{\mathbf{d}}\right)$ for $\hat{\mathbf{d}}$ along x, y and z direction, respectively. The results are shown in FIG. 5. For x and y orientations the band gaps exist, while for z orientation the band gap disappears. This can be attributed to the fact that in the PC slabs with air holes, the TE-like modes[45] with electric field parallel to the slab plane (x-y plane) have the band gaps, and the TM-like modes with electric field perpendicular to the slab plane (z direction) have no band gap. So, when the dipole is along z direction, only the TM-like modes contribute to the PLDOS and then no gap inhibition effect appears. This indicates that the SE lifetime of the quantum dot in the PC slab strongly depends on the orientation of the dipole due to pseudo band gap effect.

B. The CQED in photonic crystal L3 cavity

We now turn to investigate the CQED in the PC L3 cavity sample in Ref.11, as shown in FIG. 6(a). In this sample, the refractive index of GaAs is n=3.4, the lattice constant a=300nm, the slab thickness 0.9a and air-hole radius 0.27a. This PC L3 cavity is made by missing three air holes in a line and displacing two air holes at both cavity edges by 0.2a. The quantum dot's lifetime in GaAs without PC pattern is 1.82ns[11].

$M\left(\mathbf{r}_0, \omega, \hat{\mathbf{d}}\right)$ in FIG. 6(b) calculated by Pade approximation can be very well fitted by Lorentz function of Eq.(10). We can obtain the characteristic parameters of the coupled system: the normalized frequency of the cavity mode is $\omega_c = 0.2433232$, the quality factor Q=140398, the g factor g=22.1GHz, the vacuum Rabi splitting 44.1GHz. They are in good agreement with experimentally observed values[11], except for the calculated quality factor being about 8 times larger than the experimental Q. To understand this disagreement, we have recalculated the quality factor of some PC L3 cavities in various references[47, 48], and found excellent agreement with those calculated by other numerical methods. The disagreement between theoretical and experimental values of the quality factor may be attributed to the fabrication imperfection of the PC L3 cavity[49]. The further investigation about the effect of the fabrication imperfection on the CQED will be presented elsewhere. It is noticed that as long as $[\kappa/2|g_c(\mathbf{r}_0)|]^2 \ll 1$, the disagreement of the quality factor between theoretical and experimental values brings about a tiny change in vacuum Rabi splitting according to Eq.(12).

IV. CONCLUSION

In summary, the local coupling theory based upon the PLDOS has been constructed to simultaneously treat the SE and CQED in both the weak and strong coupling regimes. A flexible and efficient method is developed to map out the PLDOS in

arbitrary nanostructures. Based upon the *ab-initio* PLDOS, the recent experimental results about the PC slabs are very well interpreted, while the scaling invariant law is not applicable for the PC slabs to explain the experimental observations. The orientation of transition dipole moment has a profound influence on the SE of a quantum dot in the PC slabs, and no gap inhibition effect exists when the transition dipole moment is normal to the slab (z-direction). More importantly, we have established a linking bridge between the PLDOS and the CQED by the LCS to directly determine the quality factor, g factor and vacuum Rabi splitting. The measured results in the pioneering experiment about the solid-state strong-coupling system consisting of a quantum dot and the PC L3 cavity are reproduced from the *ab-initio* PLDOS. Our work enriches the knowledge about the light-matter interaction in nanostructures, and can provide guidance to tailoring the light-matter interaction at the nanoscale.

ACKNOWLEDGEMENT

This work was financially supported by the National Basic Research Program of China (2010CB923200), the National Natural Science Foundation of China (Grant U0934002), and the Ministry of Education of China (Grant V200801).

---

* Corresponding author: wangxueh@mail.sysu.edu.cn

† Present address: College of Physics Science and Information Engineering, Jishou University, Jishou 416000, China

‡ Present address: College of Science, South China Agriculture University, Guangzhou 510642, China

---

REFERENCES

[1] E. M. Purcell, Phys. Rev. **69**, 681 (1946).

[2] D. Kleppner, Phys. Rev. Lett. **47**, 233 (1981).

[3] P. Goy, J. M. Raimond, M. Gross, and S. Haroche, Phys. Rev. Lett. **50**, 1903 (1983).

[4] E. Yablonovitch, Phys. Rev. Lett. **58**, 2059 (1987).

[5] S. John, Phys. Rev. Lett. **58**, 2486 (1987).

[6] E. P. Petrov, V. N. Bogomolov, I. I. Kalosha, and S. V. Gaponenko, Phys. Rev. Lett. **81**, 77 (1998).

[7] P. Lodahl, A. Floris van Driel, I. S. Nikolaev, A. Irman, K. Overgaag, D. Vanmaekelbergh, and W. L. Vos, Nature **430**, 654 (2004).

[8] S. Noda, M. Fujita, and T. Asano, Nature Photonics **1**, 449 (2007).

[9] D. Englund, B. Shields, K. Rivoire, F. Hatami, J. Vuckovic, H. Park, and M. D. Lukin, Nano Lett. **10**, 3922 (2010).

[10] M. R. Jorgensen, J. W. Galusha, and M. H. Bartl, Phys. Rev. Lett. **107**, 143902 (2011).

[11] T. Yoshie, A. Scherer, J. Hendrickson, G. Khitrova, H. M. Gibbs, G. Rupper, C. Ell, O. B. Shchekin, and D. G. Deppe, Nature **432**, 200 (2004).

[12] K. Hennessy, A. Badolato, M. Winger, D. Gerace, M. Atature, S. Gulde, S. Falt, E. L. Hu, and A. Imamoglu, Nature **445**, 896 (2007).

[13] D. Englund, A. Faraon, I. Fushman, N. Stoltz, P. Petroff, and J. Vuckovic, Nature **450**, 857 (2007).

[14] M. Nomura, N. Kumagai, S. Iwamoto, Y. Ota, and Y. Arakawa, Nature Physics **6**, 279 (2010).

[15] J. Claudon, J. Bleuse, N. S. Malik, M. Bazin, P. Jaffrennou, N. Gregersen, C. Sauvan, P. Lalanne, and J.-M. Gerard, Nature Photonics **4**, 174 (2010).

[16] L. Sapienza, H. Thyrrestrup, S. Stobbe, P. D. Garcia, S. Smolka, and P. Lodahl, Science **327**, 1352 (2010).

[17] X.-H. Wang, R. Wang, B.-Y. Gu, and G.-Z. Yang, Phys. Rev. Lett. **88**, 093902 (2002).

[18] X.-H. Wang, B.-Y. Gu, R. Wang, and H.-Q. Xu, Phys. Rev. Lett. **91**, 113904 (2003).

[19] R. Sprik, B. A. v. Tiggelen, and A. Lagendijk, Europhysics Letters **35**, 265 (1996).

[20] K. Busch and S. John, Phys. Rev. E **58**, 3896 (1998).

[21] M. D. Birowosuto, S. E. Skipetrov, W. L. Vos, and A. P. Mosk, Phys. Rev. Lett. **105**, 013904 (2010).

[22] V. Krachmalnicoff, Castani, eacute, E., Y. De Wilde, and R. Carminati, Phys. Rev. Lett. **105**, 183901 (2010).

[23] M. Frimmer, Y. Chen, and A. F. Koenderink, Phys. Rev. Lett. **107**, 123602 (2011).

[24] Q. Wang, S. Stobbe, and P. Lodahl, Phys. Rev. Lett. **107**, 167404 (2011).

[25] H. Walther, B. T. H. Varcoe, B.-G. Englert, and T. Becker, Reports on Progress in Physics **69**, 1325 (2006).

[26] A. Faraon, I. Fushman, D. Englund, N. Stoltz, P. Petroff, and J. Vuckovic, Nat Phys **4**, 859 (2008).

[27] Y. Sato, Y. Tanaka, J. Upham, Y. Takahashi, T. Asano, and S. Noda, Nat Photon **6**, 56 (2012).

[28] M. O. Scully and M. S. Zubairy, *Quantum Optics* (Cambridge, 1997).

[29] O. J. F. Martin, C. Girard, D. R. Smith, and S. Schultz, Phys. Rev. Lett. **82**, 315 (1999).

[30] R. Wang, X.-H. Wang, B.-Y. Gu, and G.-Z. Yang, Phys. Rev. B **67**, 155114 (2003).

[31] J.-F. Liu, H.-X. Jiang, C.-J. Jin, X.-H. Wang, Z.-S. Gan, B.-H. Jia, and M. Gu, Phys. Rev. A **85**,

015802 (2012).
[32] C. Hermann and O. Hess, J. Opt. Soc. Am. B **19**, 3013 (2002).
[33] A. F. Koenderink, M. Kafesaki, C. M. Soukoulis, and V. Sandoghdar, J. Opt. Soc. Am. B **23**, 1196 (2006).
[34] C. Shen, K. Michielsen, and H. De Raedt, Phys. Rev. Lett. **96**, 120401 (2006).
[35] S. Wang and X.-H. Wang, Phys. Rev. Lett. **101**, 078901 (2008).
[36] V. S. C. Manga Rao and S. Hughes, Opt. Lett. **33**, 1587 (2008).
[37] O. J. F. Martin and N. B. Piller, Phys. Rev. E **58**, 3909 (1998).
[38] P. T. Kristensen, J. Mørk, P. Lodahl, and S. Hughes, Phys. Rev. B **83**, 075305 (2011).
[39] H. Takeda and S. John, Phys. Rev. A **83**, 053811 (2011).
[40] Y. Zhang, W. Zheng, M. Xing, G. Ren, H. Wang, and L. Chen, Optics Communications **281**, 2774 (2008).
[41] J. M. McMahon, S. K. Gray, and G. C. Schatz, Phys. Rev. B **82**, 035423 (2010).
[42] N. N. Potravkin, I. A. Perezhogin, and V. A. Makarov, Phys. Rev. E **86**, 056706 (2012).
[43] P. B. Johnson and R. W. Christy, Phys. Rev. B **6**, 4370 (1972).
[44] C. F. Bohren and D. R. Huffman, *Absorption and Scattering of Light by Small Particles* (Wiley, New York, 1983).
[45] J. Joannopoulos, S. Johnson, J. Winn, and R. Meade, *Photonic crystals: molding the flow of light* (Princeton University Press, 2008).
[46] L. C. Andreani and M. Agio, Quantum Electronics, IEEE Journal of **38**, 891 (2002).
[47] Y. Akahane, T. Asano, B.-S. Song, and S. Noda, Nature **425**, 944 (2003).
[48] Y. Akahane, T. Asano, B.-S. Song, and S. Noda, Optics Express **13**, 1202 (2005).
[49] F. Wenjuan, H. Zhibiao, L. Zheng, Z. Yunsong, and L. Yi, Lightwave Technology, Journal of **28**, 1455 (2010).

FIGURES AND CAPTIONS

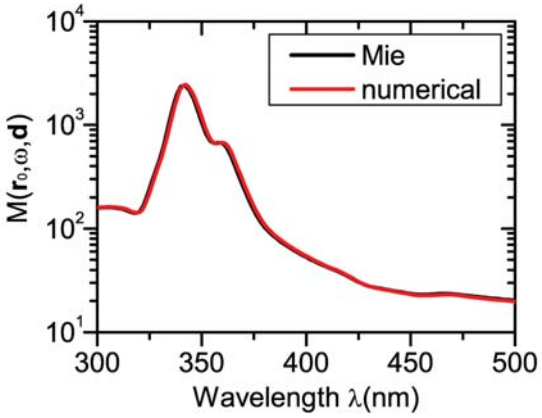

FIG. 1. Multiplication factor of the PLDOS in the vacuum with a single silver nanosphere, calculated by Mie scattering theory and our numerical method, respectively.

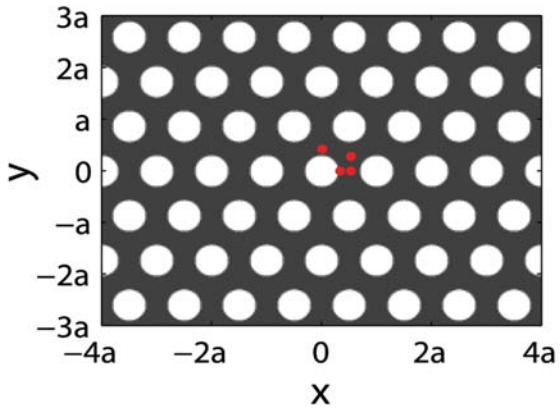

FIG. 2. Cross-section on central plane (z=0 plane) of the PC slabs. Gray region is dielectric slab and white regions are air holes.

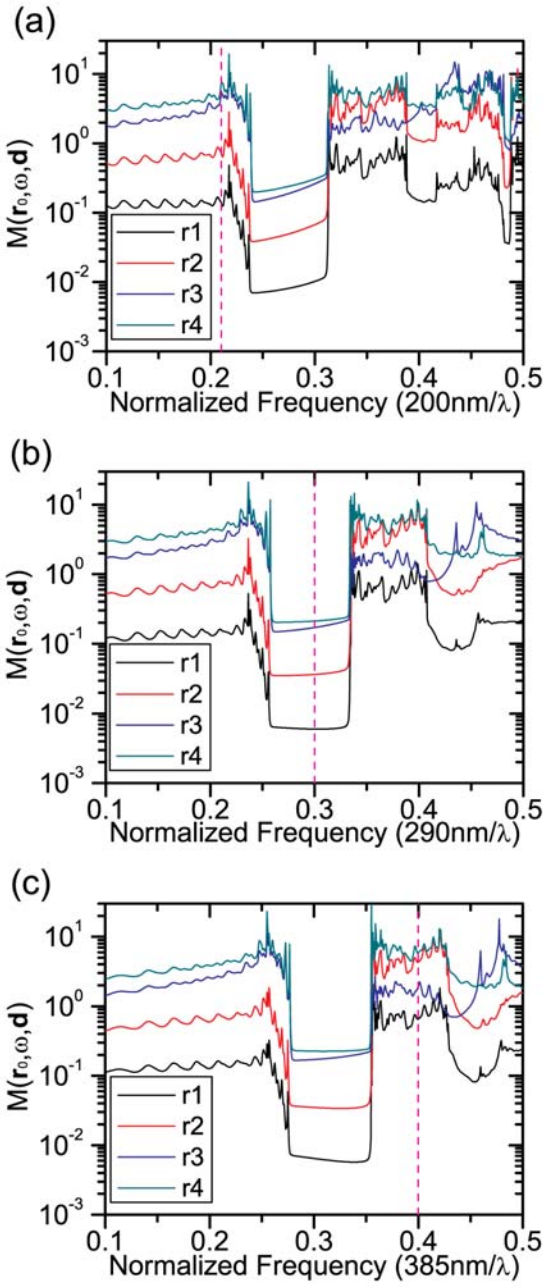

FIG. 3. $M\left(\mathbf{r}_0,\omega,\hat{\mathbf{d}}\right)$ for x-direction $\hat{\mathbf{d}}$ in three PC slabs with different lattice constant: (a) a=200nm, (b) a=290nm and (c) a=385nm. The four positions are respectively r1=(0.325a, 0, 0), r2=(0.475a, 0, 0), r3=(0.525a, 0.3a, 0) and r4=(0.025a, 0.4a, 0), denoted as red dots in FIG. 2. The vertical magenta dash lines denote transition wavelength (970nm) of the quantum dot.

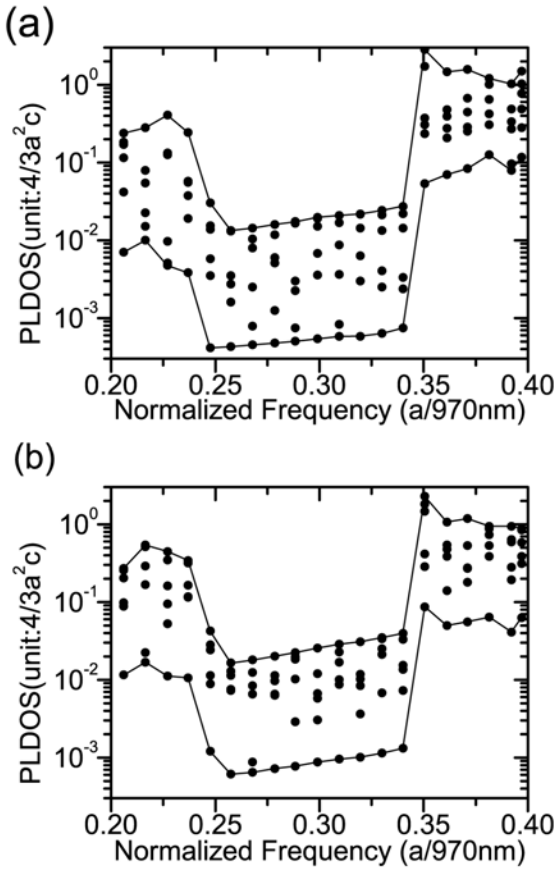

FIG. 4. The PLDOS at transition wavelength in PC slabs with different lattice constants for (a) x orientation and (b) y orientation.

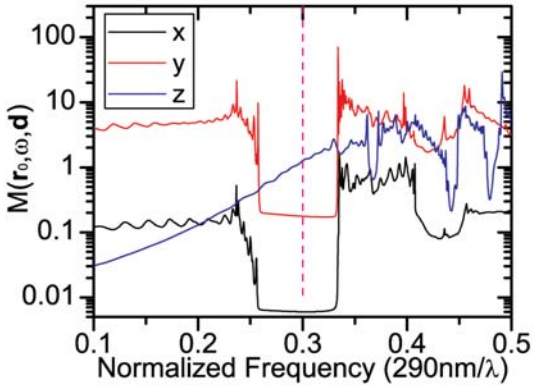

FIG. 5. $M\left(\mathbf{r}_0,\omega,\hat{\mathbf{d}}\right)$ in the PC slab with a=290nm. $\mathbf{r}_0$ is (0.325a, 0, 0). $\hat{\mathbf{d}}$ is along x, y and z direction, respectively.

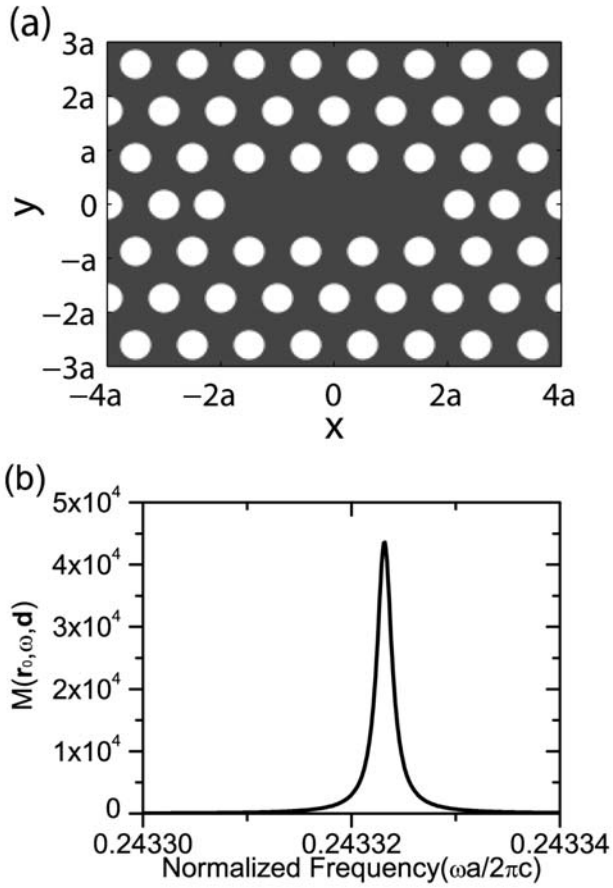

FIG. 6. (a) Cross-section on central plane (z=0 plane) of the PC L3 cavity. Gray region is dielectric slab and white regions are air holes. (b) $M\left(\mathbf{r}_0,\omega,\hat{\mathbf{d}}\right)$ in the PC L3 cavity. $\mathbf{r}_0=(0,0,0)$ is the cavity center. $\hat{\mathbf{d}}$ is along y direction.